International Journal of Mechanical, Industrial and Aerospace Sciences
ISSN: 2517-9950
Vol:6, No:8, 2012

Impact of Scale on Rock Strength

Roland Pusch, Richard Weston

***Abstract*—**The scale dependence of the strength of virtually homogeneous rock is usually considered to be insignificant but the spectrum of discontinuities plays a very important role for the strength of differently sized rock elements and also controls the rock creep strain. Large-scale load tests comprised recording of the creep strain rate that was found to be strongly retarded and negligible for stresses lower than about 1/3 of the failure load. For higher stresses creep took place according to a log time law representing secondary creep that ultimately changed to tertiary creep and failure

***Keywords*—**About four key words or phrases in alphabetical order, separated by commas

I. BACKGROUND

A. Scope of Study

THE scope was to conduct a pilot study of the scale dependence of rock strength and to examine if and how f loading of a large, apparently homogeneous rock volume can give information of this issue and on the evolution of creep strain at different stress levels.

B. Rock Strength

1. General

The stability of bored holes and tunnels is primarily determined by the compressive strength of the rock material. Under certain conditions respecting the ratio of the primary horizontal rock stresses the tensile strength can also be a determinant of the stability, as when there is a radial internal pressure on the borehole walls caused by very dense smectite clay surrounding canisters with highly radioactive waste in the hole. The unconfined compressive strength and the tensile strength of small undisturbed samples are practical standard measures of the rock material and there are detailed instructions for determining them in the laboratory. They serve as parameters of several rock classification systems for practical use and refer to defined sample sizes, usually smaller than one cubic decimeter1 [1]. For certain purposes, larger samples are sometimes tested but there are no standards or descriptions of the procedure and techniques for blocks of cubic meter size or bigger.

R. Pusch is a Professor at Luleå University of Technology, Luleå, SE-97187 Sweden, He is also with Geodevelopment International AB/Drawrite AB, Lund, Sweden (e-mail: drawrite.se@gmail.com).

R. Weston, He is in division of Production and Mechanical Engineering, University of Lund, Sweden.

[1]Standardized testing EN 1926 (Compression of cubical samples 50x50x50 mm or cylindrical ϕ 50 mm/height 50 mm), and EN 12372 (bend/tension of beams 50x50x300 mm).

[2]Typical values are 150-300 MPa for ganite and gneiss and 300-500 MPa for diabase.

This is because the strength of big rock units is primarily determined by the strength of the discrete weaknesses and their frequency, organization and orientation. When being big enough the blocks fall apart without any external forces, the critical size ranging between a cubic meter and some 1000 cubic meters Fig. 1.

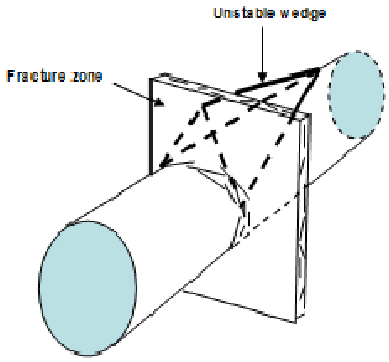

Fig. 1 Unstable wedge kept in position by forces acting in the fractures forming boundaries [1]

The current question is how relevant the compressive strength really is for predicting the stability of the rock in which large-diameter holes have been bored, like those planned to be made in the underground repository for highly radioactive waste (HLW) in Sweden. The concept implies that the holes will be vertical with 1.9 m diameter and about 8 m depth at about 400 m depth in granite where the primary horizontal stress is 30-40 MPa and the vertical stress 10-15 MPa. Calculation of the hoop stress gives values up to 150 MPa, which is ¾ to half the compressive strength of rock samples from this depth[2]. When the heat-producing waste has been placed in the holes the thermal impact increases the hoop stress by about 100 %, hence causing failure of all the holes if the swelling pressure exerted by the "buffer clay" placed between the hot canisters and the rock is not sufficient to provide adequate support. The problem is if the supporting clay has not matured sufficiently because of limited access to water from the very tight rock. The rock stresses can then cause spalling and increase in hoop stress also because of overlap of stress fields from neighbouring holes. For evaluating and considering the stability of the rock in such cases one needs to determine the stress situation on site.

2. A basic case

We will examine the case of intersection of a TBM-drilled tunnel and a deposition hole for a HLW canister, Fig. 2. The primary rock stresses are 30 MPa in X-direction, 15 MPa in Y-direction and 10 MPa in Z-direction. The calculation is based on the E-modulus E5 MPa and Poisson's ratio 0.3.

The derived principal stresses at the intersection are shown in Fig. 3.

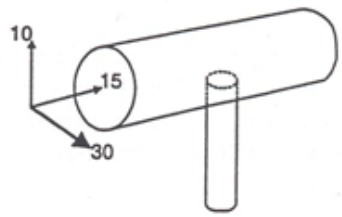

Fig. 2 bSchematic picture of a bored repository tunnel with 5 m diameter and about 8 m deep canister deposition hole with 1.7 m diameter extending from it. The highest primary rock stress 30 MPa is horizontal and oriented perpendicularly to the tunnel axis

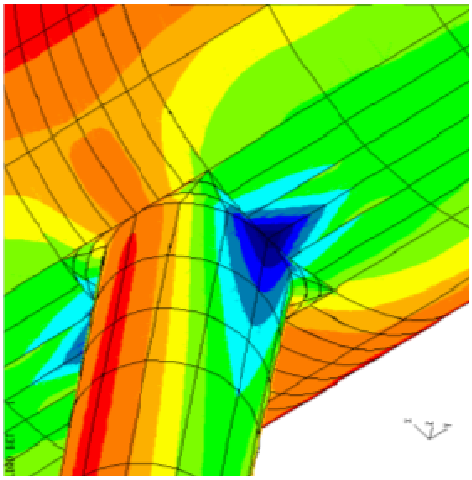

Fig. 3 Close-up view of the major principal stress plotted on the surface of the tunnel (big object) near the intersection (BEASY code). Dark-blue zone 180-206 MPa, median-dark blue zone 150-170 MPa, light-grey zone 120-130 MPa, light-blue zone 115-120 MPa, green zone 70-110 MPa, yellow zone 50-60 MPa, red zone <20 MPa. (Based on work by Computational Mechanics Center, UK)

The graph in Fig. 3 shows two important facts. Firstly, the highest hoop stress is about 206 MPa at the intersection of the hole and tunnel, which is on the same order as the uniaxial compressive strength of good crystalline rock, implying risk of failure by spalling and slabbing. Secondly, nearly constant high stresses persist within a few decimetres distance from the intersection, meaning that failure by overstressing will involve a much larger volume than just the interface of the hole and tunnel. The hoop stress drops at increased distance from the periphery of the hole but remains largely constant within 10-20 cm distance, which means that the average compressive strength of rock elements with 125 to 1000 cm3 size become exposed to nearly the same uniaxial compressive stress as at the periphery of the holes. If these larger element volumes have lower strengths the risk of failure would be obvious. Fracturing of the rock can lead to a significantly increased hydraulic conductivity in the tunnel floor and in the upper part of the hole [2].

3. Impact of specific structural features of significant persistence

For estimating the impact of natural weaknesses in the rock one can use categorization schemes for defining them and we will refer to the one shown in the Appendix to this paper. We will be concerned with discontinuities of 4th and 5th order discontinuities and show that they can have a very significant impact on the tightness and stability of repository rock. A common example is the case shown in Fig. 4, i.e. with fractures that are subparallel to large bored holes and tunnels and located close to them. One realizes that fractures of this sort, which are in fact common, can cause spalling and practically important fine-fracturing of the rock adjacent to the deposition hole, hence creating pathways for water and radionuclides that can be released from the waste container.

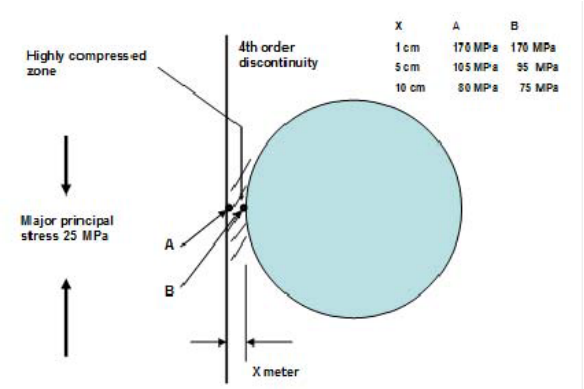

Fig. 4 Compression of thin rock slab formed between a long fracture and a 1 m canister deposition hole. For distances (x) smaller than a few centimetres breakage can take place depending on the compressive strength of the rock. Calculations by Computational Mechanics Institute (CMI), Southampton, UK

II. Fracture Mechanics

A. Failure Mechanisms

On increasing the stress level sufficiently much in rock, the smallest weaknesses in the rock matrix, termed 7th order discontinuities here [1], cf. Appendix, initiate the evolution of breakage of the virgin crystal matrix that can lead to macroscopic failure. Where there are natural discontinuities of 5th and 6th orders, representing fissures and fine fractures with small persistence, these react earlier than the crystal matrix since they are weaker, hence illustrating scale-dependence of strength. In a rock volume that is large enough to contain 4th order discontinuities, which are discrete water-bearing fractures of 10-100 m length, these are even weaker and are the ones that control the development of bulk failure. The problem of predicting fracture growth from the smallest weaknesses, voids and microfissures, and from discrete discontinuities of lower order, has been treated by numerous investigators using numerical methods for determining the stress state in 3D rock structure (Fig. 5).

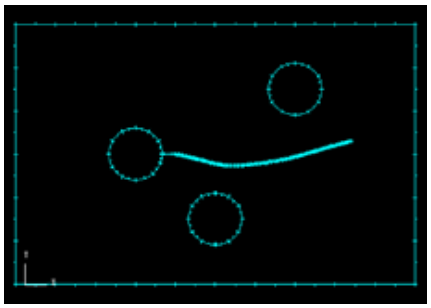

Fig. 5 Example of 2D boundary element model of rock with holes representing 7th order discontinuities. The fracture growth can be modelled by BEM technique without internal mesh generation. Only the boundary is defined (BEASY software), [3].

The detailed mechanisms causing propagation of fine weaknesses is illustrated in Fig. 6, showing the development of small defects to become oriented in directions that depend on the local stress fields.

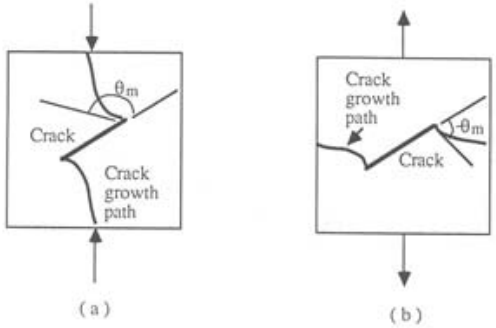

Fig. 6 Growth of plane weaknesses like elongated voids and fissures [4]

B. Experimental

Experimental strength data reflect the influence of all the discontinuities contained in the rock volume considered and since the failure mode is scale-dependent the strength is also depending on the rock volume. Thus, while the crystal matrix breaks in a brittle fashion with the initial failure taking place in the form of cleavage in the load direction, i.e. in the direction of the major principal stress, larger samples break along discontinuities or by propagation of discontinuities. It is therefore not really relevant to refer to cohesion and internal friction of the rock material: for small volumes the strength of which is best expressed by the unconfined (uniaxial) compressive strength, while for larger volumes the fracture topography (asperities) and coatings (chlorite, micas, epidote) - and above all - the pressure normal to the fractures, determine the strength. Logically, the uniaxial compressive strength is also a function of the size of the rock sample, which has been validated by systematic loading tests [5]. For granitic rock the following expression has been derived for the impact of the diameter d of cylindrical samples on the compressive strength expressed as in (1).

$$\sigma_c = \sigma_{c50}\,(50/d)^{0.18} \qquad (1)$$

Where: σ_{c50} = uniaxial compressive strength of a core sample with 50 mm diameter and height.

This relationship implies that a 200 mm diameter sample has a strength that is only 80 % of one with 50 mm diameter. Naturally, the strength of larger rock volumes drops further as vizualised in Fig. 7.

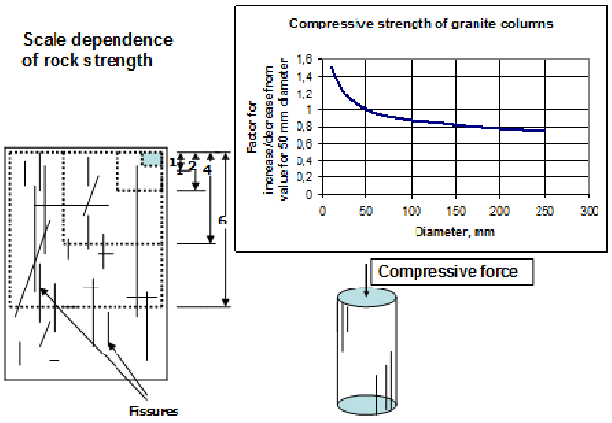

Fig. 7 Influence of size of sample with one type of defects on the compressive strength. The drop in strength at increased volume is explained by the increasing number of defects and the greater possibility of critical orientation and interaction of the defects [1].

C. Semi-Empirical Modelling

1. Granite-Based Data

Application of (1) gives the compressive strength reduction factor σ_x / σ_c c (volume x=$\pi d^3/4$ in cm^3 in Table 1 (Model 1). This table also gives literature-derived data [6], which, using Weibull statistics and taking 100 cm3 as reference volume, gave data according to Model 2.

Model 1 implies that the strength of a 1 m^3 (E6 cm^3) block of rock with no discernible macroscopic weaknesses is 65 % of that of a 100 cm3 homogeneous block while it is 33 % according to Model 2. Averaging these data one can estimate that the big block has half the strength of the small one.

Turning back for the moment to Fig. 3, which demonstrates that critical stability conditions will prevail within 10-20 cm distance from the intersection of the hole and tunnel under the assumed primary rock stresses, one concludes that unstable conditions may appear in the entire tunnel floor and down to a couple of meters depth in the deposition holes.

TABLE I
STRENGTH REDUCTION FACTOR σX/σC (VOLUME X=πD3/4 IN CM^3)

Volume, cm^3	Model 1	Model 2
1	1.50	3.30
10	1.20	1.70
100	1.00	1.00
1000	0.85	0.67
10000	0.75	0.50

100000	0.70	0.40
1000000	0.65	0.33

Failure by spalling is expected associated with increased hydraulic conductivity of the rock.

2. Bjärlöv Granite

Pink granite from north-eastern Skåne, the southernmost county in Sweden, has long been used for manufacturing of curbstone and for lining floor and walls of buildings, and artists have prepared a number of famous sculptures from it. Compression tests on core samples with 26 mm diameter has given a compressive strength of 180-250 MPa and beam tests have shown the tensile strength to be one tenth of the compressive strength, i.e. at least 18 MPa. Application of the theoretical models for the impact of scale would imply an average compressive strength of 90-125 MPa and a tensile strength of 9-13 MPa of elements with a volume of 0.25-1 m^3.

III. Full-Scale Tests On Bjärlöv Granite Columns

A. General

The Bjärlöv granite is unweathered and has a sufficiently low content of 5th and 6th order discontinuities to allow extraction of parallel-epipedic blocks with up to 10 m length. Breivik's columns were 6 m tall and had 30cmx40cm cross section. They contained 10 to 20 cm wide pegmatite bands, which did not cause failure.

The columns were shaped to have consoles for carrying a large glass roof and the bending moment generated by its weight was concluded to give too high stresses to guarantee stable conditions. The designer, the Norwegian consulting company Instanes A/S therefore required strengthening by drilling an axial, centrally placed hole for a steel rod that was preloaded to give a net compressive stress.

One of the columns did not have any steel anchor and was used for determining the strength and stress/strain properties by performing load tests with the column placed horizontally as a beam.

B. Test Set-up

The load test was made by placing the 560 cm long column horizontally on supports at the ends and applying point loads in two positions Fig. 8.

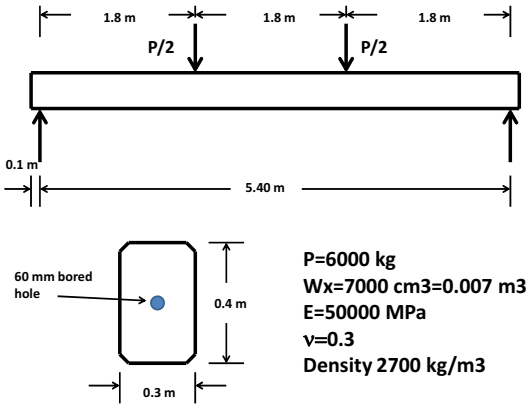

Fig. 8 Test arrangement

The P/2 loads were applied via a centrally loaded DIP 200 steel beam. The loading was made by keeping the hydraulic pressure in the centrally placed jack constant during each load step of 16 kN. The deflection was recorded for 10 minutes for getting information on the early creep strain. Unloading was made at the end of each pressure step.

C. Predictions

1. Stress Distribution and Deflection

Analytically the beam would be exposed to a maximum bending moment of (90P +8800) Nm, a maximum tensile stress of (0.01186P + 1.26) MPa, and a maximum deflection of about 6PxE-7 m for P in N. For the actual load constellation the about 200 000 cm3 large central part of the beam would be exposed to the same tensile stress. Had the tensile strength been the same as for the 100 cm^3 core samples, i.e. at least 18 MPa, the failure load P would be 130 kN. A load P=62 kN (6200 kg), which turned out to be the true failure load, would yield a maximum tensile stress of 8.58 MPa and a deflection of 3.7 mm for the assumed E-modulus.

FEM calculation of the stress distribution in the rock column gave the diagram in Fig. 9 for P = 62 kN (6200 kg), with the maximum tensile stress 8.11 MPa and maximum deflection 2.6 mm. These values are in reasonable agreement with the analytically derived ones. The graph shows that the tensile stress was largely constant in the central third of the beam length, involving a volume of about 50000 cm^3.

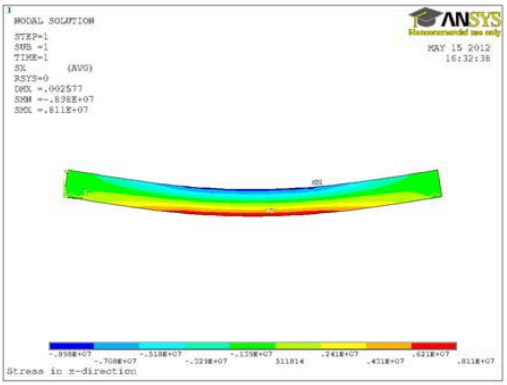

Fig. 9 Stress distribution in the beam according to the FEM analysis

D. Measurements

The deflection of the beam is shown in Fig. 10, which indicates that the granite beam behaved largely elastically up to P=62 kN (6200 kg).

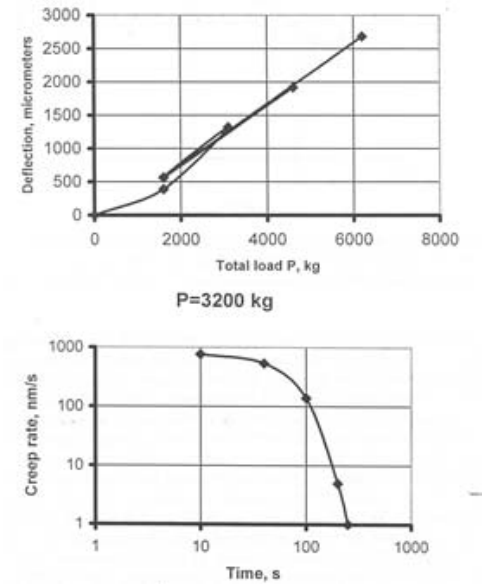

Fig. 10 Load versus deflection. The upper diagram shows that the beam behaved almost elastically up to the maximum load that could be applied. The lower diagram shows that the creep strain for the fourth load step P=32 kN (3200 kg) dropped very quickly in about one minute. The preceeding loads gave even quicker retardation.

Fig. 11 shows that creep was more obvious for higher loads. For P=4800 kg it dropped with time but was still obvious after 10 minutes, while failure, manifested by rapid "tertiary" creep, took place for P=62 kN (6200 kg).

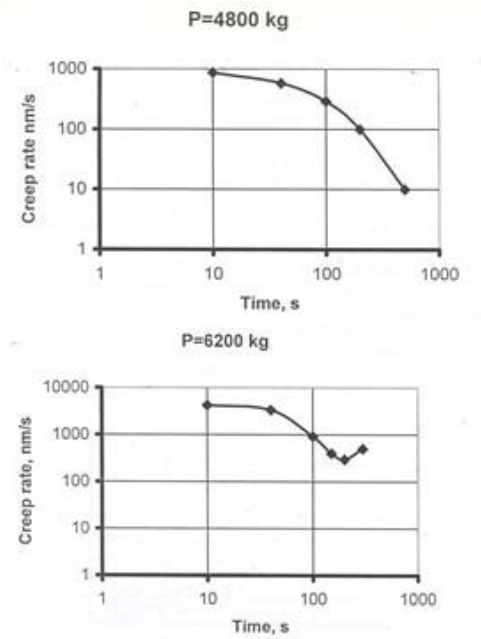

Fig. 11 Creep rates for P=48 kN (4800 kg) in the upper diagram and 62 kN (6200 kg) in the lower. For the firstmentioned load the creep rate was still obvious after 10 minutes and for the lastmentioned load "tertiary" creep started soon after load application and led to failure after a couple of minutes.

IV. Discussion And Conclusion

A. Agreement between Predictions and Actual Behavior

The tests demonstrated that the granite beam of which about one third, i.e. around a quarter of a cubic meter (240 000 cm^3), had actively carried the applied load exhibiting elastic behavior but failed at a tensile stress of about 8.6 MPa. This demonstrates that the expected tensile strength, around 20 MPa, was not reached and that the difference shall be taken as a measure of the scale dependence of rock strength. It is interesting to see that the strength reduction according to Models 1 and 2 in Table 1 give an average drop by about 40 % for an increase in sample volume from 100 to 50000 cm3, indicating that the scale effect is a true phenomenon and that the reduction of rock strength is on the order of magnitude implied by the models.

B. Progressive Failure of Rock

Progressive failure results from local overstressing and accumulation of slip units much in the way that we imagine creep strain to take place. For materials characterized by a spectrum of bond strengths the heterogeneity in stress and structure on the microscale, exemplified by geological matter, jointly result in a distribution of heights of the energy barriers. Thermal activation is nearly always observed, more for soft, ductile matter like soils, than for hard, brittle material like rock. Common to both is, however, that in given points in the materials slip on the molecular scale is held up at an energy barrier that is determined by the intrinsic nature of the obstacle as well as by the local deviatoric stress acting on it at a certain time.

For soils the barriers are represented by interparticle bonds of various types, the highest represented by cementing bonds and primary valence bonds and the lowest by van der Waals and hydrogen bonds. For the crystal matrix of rock they stem from strong chemical bonds and primary valence bonds. Taking the asperities in natural discontinuities to represent slip units comparable to those made up of yielding particle aggregates in soils Fig. 12 one can apply a thermodynamically based creep theory that is common to both material types [7].

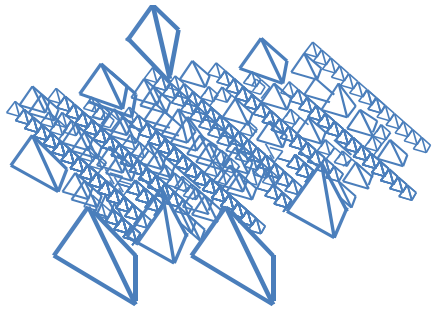

Fig. 12 Schematic appearance of asperities in discontinuities of high orders in granitic rock. Three sizes represent different barrier heights of the energy spectrum, the biggest asperities represent the highest barriers to slip

C. Creep Strain

Creep theories based on thermodynamics have different forms for low-stress cases representing largely unchanged microstructural constitution, i.e. primary creep, and cases implying microstructural damaging (secondary and tertiary creep) [1, 7]. For the first cases strain is of the type:

$$\varepsilon=\alpha(t)-\beta(t^2) \text{ with the conditions } (t<\alpha/2\beta) \quad (2)$$

While for the second case it has the following mathematical form:

$$\varepsilon=B\ln(t+t_o)+A \quad (3)$$

Where: t is time after onset of strain and α, β, A and B material constants that depend on the microstructural build-up, stress history, mineralogical composition, stress level, and temperature.

For the beam creep took place according to 2 when the load was about 1/3 of the failure load, and according to Eq.2 when it was about 2/3 of the failure load. For the failure load the creep rate followed initially as in 3 but the accumulated strain led to so much microstructural damage that total failure occurred quickly. This test indicates that a safety factor of 3 is required for providing long-term stability.

D. Practical Consequences

An example of the consequences of the scale-dependence of rock strength is that large boreholes, like the large-diameter deposition holes with 8 m depth for hosting heat-producing canisters with highly radioactive waste in SKB's a repository in rock, will fail by spalling at significantly lower hoop stresses than the laboratory-scale compressive strength of small test samples on which the design was based.

APPENDIX

TABLE II
CATEGORIZATION SCHEME FOR ROCK DISCONTINUITIES

Geometry				Characteristic properties		
Order	Length, m	Spacing, m	Width, m	Hydraulic conductivity	Gouge content	Shear strength
Low-order (conductivity and strength refer to the resp. discontinuity as a whole)						
1st	>E4	>E3	>E2	Very high to medium	High	Very low
2nd	E3-E4	E2-E3	E1-E2	High to medium	High to medium	Low
3rd	E2-E3	E1-E2	E0-E1	Medium	Medium to low	Medium to high
High-order (conductivity and strength refer to rock with no discontinuities of lower order)						
4th	E1-E2	E0-E1	<E-2	Low to medium	Very low	Medium to high
5th	E0-E1	E-1 to E0	<E-3	Low	None	High
6th	E-1 to E0	E-2 to E-1	<E-4	Very low	None	Very high
7th	<E-1	<E-2	<E-5	None	None	Very high

E denotes the log scale exponent, i.e. E4=10000, E1=10, E-2=0.01 etc

ACKNOWLEDGMENT

The key part of this report deals with the strength of granite rock columns extracted from the rock at Bjärlöv, northeastern Skåne, Sweden. Raw blocks were released from the rock by careful splitting and transported to China for trimming to the desired dimensions, followed by shipping to Bergen in Norway where they were finally placed as carriers of a large glass roof over a market. The creator of the beautifully decorated columns was Bård Breivik, professor at the Academy of Art in Stockholm, Sweden, is gratefully thanked for financing the load testing. The authors are also greatly indebted to civ. Eng. Nils Bakke at Instanes A/S, Norway and to Karl-Erik Nyman, Intergrund AB, Lomma, Sweden, for valuable discussions in planning and performance of the tests.

REFERENCES

[1] Pusch, R., Yong, R.N., Nakano, M., *High-level Radioactive Waste Disposal*, WIT Press, Southampton, UK, 2011.
[2] Liedtke, L., Shao, H., Alheid, H. J., Sönnke, J., "Material Transport in Fractured Rock – Rock Characterization in the Proximal Tunnel Zone" *Federal Institute for Geosciences and Natural Resources*, Hannover, Germany, 1999
[3] Pusch, R., Adey, R., *Accurate computation of stress and strain of rock with discontinuities. Advances in Computational Structural Mechanics*, Civ. Comp. Ltd, Edinburgh, Scotland, 1998, pp.233-236.
[4] Whittaker, B.N., Singh, R.N., Sun, G., *Rock Fracture Mechanics*, Developments in Geotechnical Engineering, 71. Elsevier Publ. Co., 1992.
[5] Martin, D., "Brittle Rock Strength" *TVO & SKB Workshop*, *Nuclear Waste Management, TVO technology project*, Work Report TEKA-94.07, Helsinki, 1994.
[6] Pusch, R., *Rock Mechanics on a Geological Base*, Developments in Geotechnical Engineering, 77. Elsevier Publ. Co, 1995.
[7] Pusch, R., "Creep in rock as a stochastic process" *Engineering Geology*, Vol.20, 1984, pp.301-310.